IEEE Access
Multidisciplinary ⋮ Rapid Review ⋮ Open Access Journal

Received January 22, 2021, accepted February 1, 2021, date of publication February 16, 2021, date of current version March 3, 2021.

Digital Object Identifier 10.1109/ACCESS.2021.3059680

Segmentation of the Airway Tree From Chest CT Using Tiny Atrous Convolutional Network

GUOHUA CHENG[1], XIAOMING WU[2], WENDING XIANG[1], CHUAN GUO[3], HONGLI JI[1], AND LINYANG HE[1]

[1]Hangzhou Jianpei Technology Company Ltd., Hangzhou 310000, China
[2]The Second Affiliated Hospital Zhejiang University School of Medicine, Hangzhou 310000, China
[3]Zhejiang Integrated Traditional and Western Medicine Hospital, Hangzhou 310000, China

Corresponding author: Linyang He (he.linyang@jianpeicn.com)

This work was supported in part by the Key Research and Development Plan of the 13th Five Year Plan, Ministry of Science and Technology, China, under Grant 2016YFB1000400, in part by the Scientific Research Foundation of National Health and Family Planning Commission under Grant WKJ-ZJ-1814, in part by the Key Research and Deveopment Plan of Zhejiang Province under Grant 2019C03002, and in part by the Hangzhou Major Science and Technology Innovation Project under Grant 20172011A038.

ABSTRACT The airway tree is one of the most important part in human respiratory system. Airway segmentation plays a crucial role in pulmonary disease diagnosis, localization and surgical navigation. We propose a novel method to improve airway segmentation in thoracic computed tomography(CT) using deep learning. In order to take into account the multi-scale changes of the airway and achieve accurate airway segmentation, we design an end-to-end Tiny Atrous Convolutional Network (TACNet) based on 3D convolution neural network. In view of the difficulty of classification due to the numerous branches of airway, two evaluation factors, namely, the angle of airway bifurcation and the buffer length of airway bifurcation are designed, which are used for airway classification by combining the centerline extraction. We train TACNet on the inspirator thoracic CT scans with ground truth, which are generated by clinicians and evaluate on our own clinical data sets and EXACT'09 data sets. Compared with state-of-the-art airway segmentation algorithms, proposed algorithm in this paper achieve very competitive results in 20 test datasets of the EXACT'09 challenge. The experimental results show that the algorithm proposed in this paper has high robustness and advantages regardless of airway segmentation or airway classification. In 20 test datasets of the EXACT'09 challenge, the average airway tree length detection rate is the best in the public literatures.

INDEX TERMS Airway classification, convolutional neural network, deep learning, semantic segmentation, CT, medical image.

I. INTRODUCTION

A. BACKGROUND

Airway is an important part of human lung and a primary channel for enabling airflow between the human body and the external environment. As the lungs and airway are directly in contact with the external environment, they are inevitably affected by stimulants such as haze, pollutants, allergens, dust and chemicals in the air. Over the last few decades, the prevalence of respiratory diseases has been increasing [1]. Chronic obstructive pulmonary disease (COPD) has been predicted by WHO to be one of the leading causes of death by the year 2020 [2].

The associate editor coordinating the review of this manuscript and approving it for publication was Inãs Domingues.

The airway is a hollow cartilaginous tube generally located as a midline structure displaced slightly to the right and marks the beginning of the tracheobronchial tree. A series of airway cartilages joined together by annular ligaments provides structural integrity from collapse. At the level of the sternal angle, the airway bifurcates into the right and left main bronchi. They undergo further branching to produce the secondary bronchi. Each secondary bronchi supplies a lobe of the lung, and gives rise to several segmental bronchi. Along with branches of the pulmonary artery and veins, the main bronchi make up the roots of the lungs. The segmental bronchi undergo further branching to form numerous smaller airways-the bronchioles. Human airways appear as a treelike branching network of tubes that enable airflow into the lungs through the trachea. From the airway to the terminal bronchioles, an airway tree consists of

approximately generations of branches, beyond which alveoli begin to appear and ultimately terminate at the alveolar sacs where most gas exchange occurs [3].

As the airway tree shows unique structural characteristics, pulmonary disorders are usually associated with morphological changes in the lungs and airway [4]. The pathological changes of the airways are often accompanied by changes in the anatomical structure of the airway [5]. Therefore, information about the anatomical structure of the lungs and airway is often used in the diagnosis of pulmonary disorders and the evaluation of therapeutic effect fovariety of applications and constitutes an important part of computer-aided detection (CAD) of lung diseases in medical imagining. It enables improved objectivity and repeatability in medical image diagnosis, increase in diagnostic efficiency, and can promote the transformation of image quantitative diagnosis mode [6]. CT image segmentation of pulmonary tracheobronchial tree is the basis of pulmonary function area division and pulmonary pathological parameters measurement, and is also an important part of the application of surgical navigation. However, due to the effects of motion artefacts, imaging noise, partial volume effect and lumen mucus, the density or gray distribution of the lumen in the lung and airway is very uneven, and the end of the lumen is prone to local wall rupture, which is easy to diffuse into the pulmonary parenchyma during bronchioli segmentation. Therefore, pulmonary airway tree segmentation is a difficult research topic.

B. RELATED WORK

In recent years, there have been many automatic or semi-automatic segmentation methods of lung and airway tree based on CT images. Peng Shuangquan [7] proposed a 3D lung-airway tree segmentation method which combines region growth with morphological gray reconstruction. This method used threshold segmentation and morphological closed operation to realize lung airway tree segmentation. The method based on active contour is introduced into the segmentation of lung and trachea, and the rough segmentation results are obtained in 3D images. Then, the separated parts of the rough segmentation results are connected by gray reconstruction method. Finally, the bronchial tree is extracted by using 3D region growing. He Ruihua *et al.* [8] designed a fully automatic segmentation method for 3D bronchial tree based on active contour model. Fabija ska *et al.* [9] used two passes of 3D seeded region growing to address problem of pulmonary airways investigation based on high-resolution multi-slice spiral CT chest scan. Zijian B *et al.* [10] proposed a new machine-based learning method to extract airway and non-airway voxel samples using optimized sampling procedures, and used random forest classifier to determine whether each voxel belongs to Airway class. Irving *et al.* [11] proposed a method of airway and main bronchus segmentation based on threshold and region growth was proposed. The bronchus was accurately segmented by morphological filtering and reconstruction, and the leak was removed by edge dilation. Lo *et al.* [12] presented a method for airway tree segmentation that uses a combination of a trained airway appearance model, vessel and airway orientation information, and region growing. In EXACT'09 Pulmonary Airway Segmentation Challenge Competition, Lo *et al.* [13] proposed 15 airway segmentation algorithms, most of which are based on region growth, morphological processing, and some other medical image segmentation algorithms. Xu *et al.* [27] proposed a computational framework to accurately quantify airways through a novel hybrid approach for precise segmentation of the lumen. Lee *et al.* [29] used multi-scale filtering and support vector machine (SVM) classification to automatically segment the airway regions on 3D volume chest computed tomography (CT) scans. Lo *et al.* [31] presented a method for airway tree segmentation that uses a combination of a trained airway appearance model, vessel and airway orientation information, and region growing. Weinheimer *et al.* [32] presented a method for fully automated extraction of airways from volumetric computed tomography (CT) images based on a self-adapting region growing process. These methods based on traditional image processing have some limitations in segmentation accuracy and robustness.

In 2012, due to the proposal of AlexNet [14], deep learning began to be widely used in the field of computer vision, especially the proposition of FCN [15], U-Net [16], V-Net [17], and the application of convolutional neural network (CNN) in image segmentation appeared in large quantities. In the aspect of lung and airway segmentation, [18]–[20] and others have proposed CNN-based methods [21].

Jihye Yun *et al.* [22] designed a 2.5D-based pixel-level airway segmentation model for leak detection. The network structure improved the detection rate of airway, and the false positive rate was relatively low, but the network was realized by iteration. Charbonnier *et al.* [28] also presented a method to improve a given airway segmentation by detecting leaks in the segmented airways using ConvNets. Qin et al [33], [34] proposed AirwayNet and AirwayNet-SE mainly based on voxel-connectivity aware approach to perceive the tree-like pattern and comprehend the connectivity of airway. These methods have achieved good results in airway segmentation, but there is still room for further improvement. At the same time, these methods do not mention the realization of airway classification.

Therefore, in view of the shortcomings of existing solutions, this paper proposes a lung CT airway tree segmentation and classification method based on deep learning, and carries out experimental tests on clinical data set and EXACT'09 public data set. Quantitative evaluation is carried out by using EXACT'09 official evaluation index and Dice similarity coefficient. The number of branches detected at each level, the detection rate and the correct detection rate at segment level are given. The main structure of this paper is as follows: Section 2 mainly describes data sources and annotations; Section 3 details the segmentation and classification methods proposed in this paper; Section 4 is the experiments result; Section 5 is the conclusion.

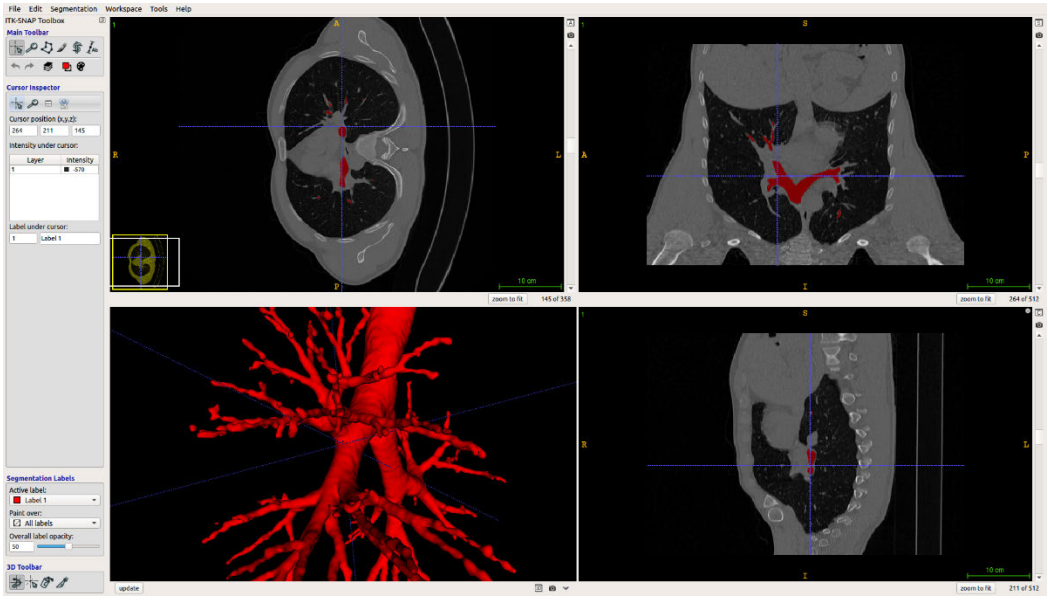

FIGURE 1. Marking Airway gold standard using ITK-SNAP.

II. DATA AND GROUND TRUTH

A. DATA

The proposed TACNet was trained and evaluated on a randomly selected set of 100 clinical thoracic CT scans and EXACT'09 challenge public dataset. Clinical datasets were collected from Shao Yifu Hospital affiliated to Medical College of Zhejiang University, Zhejiang People's Hospital and Guizhou People's Hospital in May 2016, August 2017 and October 2018, respectively. All scans were reconstructed to 512×512 matrices with DICOM format, with in-plane voxel sizes between 0.3mm and 0.65mm, slice thickness between 0.5mm and 2.0mm, aged 18-85 years, weighing 40-108 kg and clinical diagnosis included pulmonary nodules, pneumonia, bronchiectasis, pneumothorax, emphysema. The public dataset EXACT'09 officially provided 40 cases of CT data, CASE01-CASE20 for training and CASE21-CASE40 for testing. The data was obtained from different research teams, CT scanning equipment, reconstruction algorithm, radiation dose and so on. The thickness range was 0.6mm-1.25mm. In clinical dataset, 80% of the cases were randomly selected for training, 10% for validation and 10% for test.

B. GROUND TRUTH

Except for EXACT'09 data, all clinical data was subjected to semi-automatic labelling to obtain gold standard. The participants in labelling are radiologists who had worked in the radiology department for more than 10 years. ITK-SNAP [23] is the software used by radiologists to label the gold standard as shown in Figure 1. The marking is carried out in two rounds. Markers in the first round are randomly assigned. After each task is completed, all marking results are summarized. The second round is mainly to find out the areas marked in dispute. Therefore, all markers are required to make a second discrimination and pass the marking task. The voting method is used to determine these disputed areas, and finally all the marking results are summarized to obtain the final gold standard mask.

III. METHOD

The methods of airway segmentation and classification proposed in this paper include data pre-processing, airway segmentation, post-processing and airway classification as shown in Figure 2.

A. DATA PREPROCESSING

All data used in this paper are diverse, such as in the thickness of the slices. At the same time, because the volume of the overall data of lung CT images is very large and the actual computer memory capacity is limited, all data needed to be pre-processed before segmentation. The pre-processing used in this paper includes: (1) *Interpolation*: The thickness of DICOM data collected from medical imaging equipment is different in different dimensions. In order to standardize the data, it is necessary to interpolate medical data. In this paper, bilinear interpolation method is used to interpolate lung DICOM data to the smallest spacing. (2) *Lung segmentation and crop*: The main purpose of lung segmentation is to obtain the region of interest (ROI) of the lung. The bounding box is obtained according to the size of lung parenchyma in different cases. This bounding box serves as the ROI for subsequent airway segmentation. At the same time, the heart, the air area outside the body and non-pulmonary areas such as ribs were removed. (3) *Setting sliding window grids*: Considering the memory consumption of the computer, the size of input data is set as $96 \times 96 \times 96$. We use a sliding block method in each CT to obtain the input data. (4) *Data augmentation*: Data augmentation is mainly used to enhance the generalization ability of the model, while preventing model from over-fitting. Since

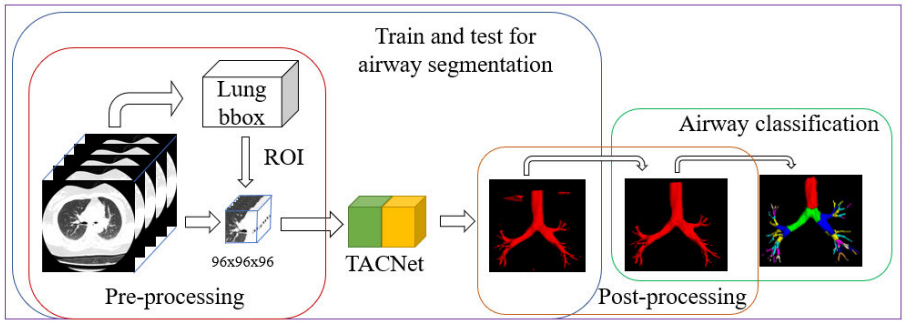

FIGURE 2. Flow chart of airway segmentation and classification.

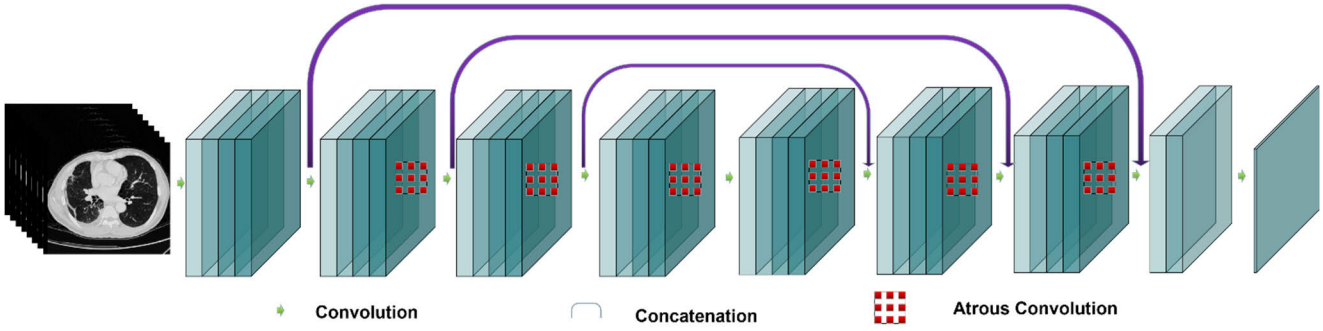

FIGURE 3. TAC network structure.

the airway branch of the lung is a tubular structure of different thicknesses and presents an inverted tree structure as a whole, the operation of translation and scaling is mainly adopted.

B. SEGMENTATION NETWORK MODEL

The name of our model is TACNet (Tiny Atrous Convolutional Network), since the main convolution operation we use in the network is Atrous convolution. The network architecture is illustrated in Figure 3. The role of Atrous convolution includes the following two aspects: (1) Enlarge the receptive field, (2) Capture multi-scale context information. Due to the tree-like structure of the airway, the size from the main trachea to the bronchi gradually decreases, as shown in Figure 4. If ordinary convolution operations and the traditional U-Net [16] network structure are used, the feature map will be down-sampled multiple times. Although the receptive field increases, it will cause the size of the feature map to decrease. Many smaller bronchi will disappear in the feature map or become no longer obvious after multiple down-sampling, so we adopted a method of Atrous convolution to adjust the network structure. The purpose is to ensure that the feature map does not shrink in size while ensuring the receptive field. Our network does not have a pooling layer during the entire design process, and TACNet maintains the original resolution after each layer as shown in Figure 3.

The proposed TACNet model consists of nine convolution layers and no pooling layers. The first layer and the last layer use $3 \times 3 \times 3$ convolution. Atrous convolution[24] kernel size $3 \times 3 \times 3$ with dilated rate of 2 is used in the second and seventh layers, and $3 \times 3 \times 3$ atrous convolution with dilated rate of 4 is used in the third and sixth layers. The

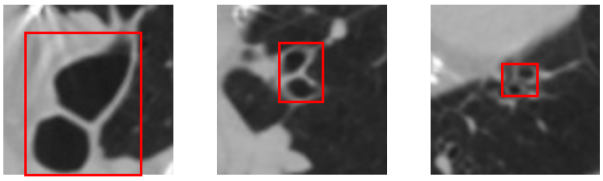

FIGURE 4. Multi-scale tracheal structure (size from large to small).

first eight layers are mainly used for feature extraction to obtain the semantic information of CT images. At the same time, a concatenation with the shadow layer feature map and the deep layer output is performed to fuse the semantic information of different scales and feed into the next layer. In particular, the output of the third layer and the output of the fifth layer are joined together as the input of the sixth layer, the output of the second layer and the output of the sixth layer are joined together as the input of the seventh layer, and the output of the first layer and the output of the seventh layer are joined together as the input of the eighth layer. The number of channels from the first layer to the seventh layer is 32, the number of channels in the eighth layer is 16, the number of channels in the ninth layer is 1, the batch regularization and a rectified linear unit (Relu) are used after each convolution layer. The input of the network is $96 \times 96 \times 96$. Because the diameter of the main airway and left and right bronchus outside the lung is larger and need larger receptive field. The dilated rate of Atros convolution is set to 8 in the sixth layer, and the remaining part remains unchanged.

C. POST PROCESSING

The results obtained by model segmentation inevitably have some non-airway regions, which are mainly due to (1) in

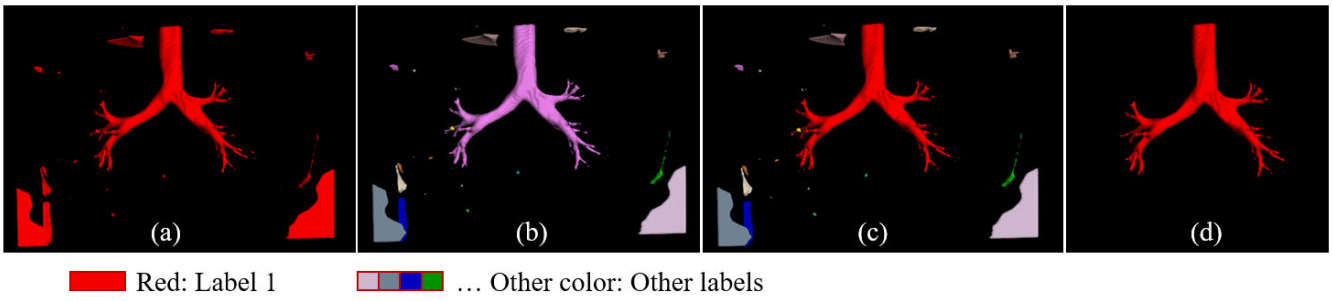

FIGURE 5. The post-processing flow.

some cases, there are different severity lesion areas in the lung, such as emphysema, bullae, etc., so the segmentation results will inevitably have isolated false positive areas; (2) part of the lung edges obtained by clipping will also be predicted as false positives which need to be removed. Therefore, a post-processing method for analyzing the connected region and extracting the largest connected region is used to obtain the final airway segmentation result.

The post-processing method mainly includes the following steps: (1) *Set a threshold on the output of TACNet to obtain the binary segmentation result.* We set threshold $t = 0.5$ in this paper. The output segmentation result of the model is a rough segmentation result that needs post-processing, as shown in Figure 5(a). This result contains many scattered or false positive areas outside the airway, which is not satisfactory. (2) *Connected region analysis.* For each connected region that is independent in three-dimensional space, we label it with a corresponding independent label. In this process, the label number is disordered. The mask of the independent connected region is shown in Figure 5(b). (3) *Sort the independent regions by volume and extract the largest connected region.* We keep the largest connected region in the three-dimensional space, and set the other parts as the background to get the final valid airway segmentation result. As shown in Figure 5(c-d).

D. CLASSIFICATION OF AIRWAY

Airway classification is mainly used to locate intrapulmonary lesions, navigate and evaluate the length and integrity of airway segmentation. Airway classification plays a vital role in both quantitative and qualitative analysis of airway branches. The airway tree is modelled mainly based on the theoretical airway segmentation models proposed in [13], [25], [26].

In this paper, the main process of airway classification is as follows:

After the previous post-processing, we got the single label segmentation result of the airway, as shown in Figure 5(d). Then we will extract the centerline of the airway to get the tree-like centerline of the airway. As shown in Figure 6(a). The centerline of the airway at this time is a connecting line composed of a single pixel.

Next, we build a tree-shaped data structure for the centerline. The set of all points on the centerline of the airway is denoted as $\boldsymbol{P}$. The initial seed point $\boldsymbol{S}$ is selected as the uppermost point of the airway in the human body coordinate system. Then we traverse the point on the centerline in the 26 neighborhoods of the seed point. (a) If there is only one child point in the current neighborhood, the child point will be labeled the same label as the seed point. (b) If there are more than two child points in the current neighborhood, the seed point will be marked as a bifurcation point, and the label of the two child points will be added one. Then the current seed point will be removed from the set $\boldsymbol{P}$, and the child point will be set as a new seed point $\boldsymbol{S}$ to continue traversing on the centerline. If there are multiple child points, they will be set as seed points respectively. The centerline classification algorithm process is shown in Figure 7. The classification result of the airway centerline after traversal is shown in Figure 6(b).

Then for all the pixels of the single-label airway, each point will be matched with the nearest neighbor on the classified centerline. When the distance between the current point and a point on the centerline is the closest, the label of current point is set as the label of the nearest neighbor on the centerline until all pixel targets are traversed. The airway tree after the traversal is shown in Figure 6(c).

In addition, two evaluation factors(*the bifurcation angle of the current airway* and *the bifurcation length of the current airway*) are introduced to refine the branch of the airway. These two evaluation factors are used to accurately determine the current branch series of the airway. The bifurcation angle of the current airway and the bifurcation length of the current airway are calculated separately.

1) THE ANGLE OF AIRWAY BIFURCATION

Bifurcation angle refers to the angle between the current branch and the previous branch. For example, in Figure 6(b), the angle $\angle P_1P_2P_3$ represents the angle between the branch in label3 and the previous branch in label2. Because the airway presents an inverted tree structure as a whole, and there are some small branches growing around the left and right bronchi, the angle between the current branch and the previous branch can be used to determine that the branch is the upper trachea.

2) THE BUFFER LENGTH OF AIRWAY BIFURCATION

Bifurcation buffer length refers to the distance between the current bifurcation point and the next bifurcation point.

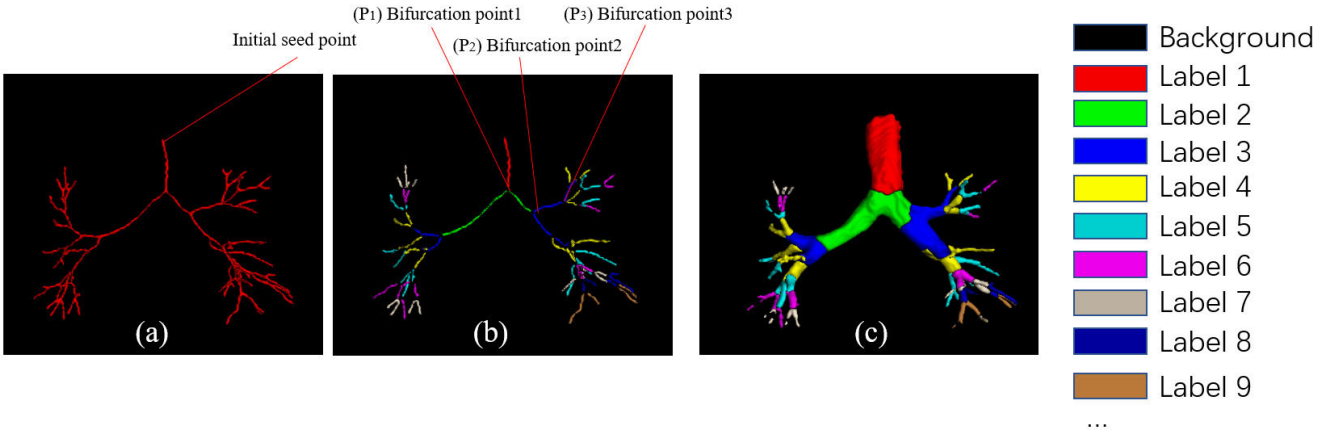

FIGURE 6. Airway centerline extraction and classification.

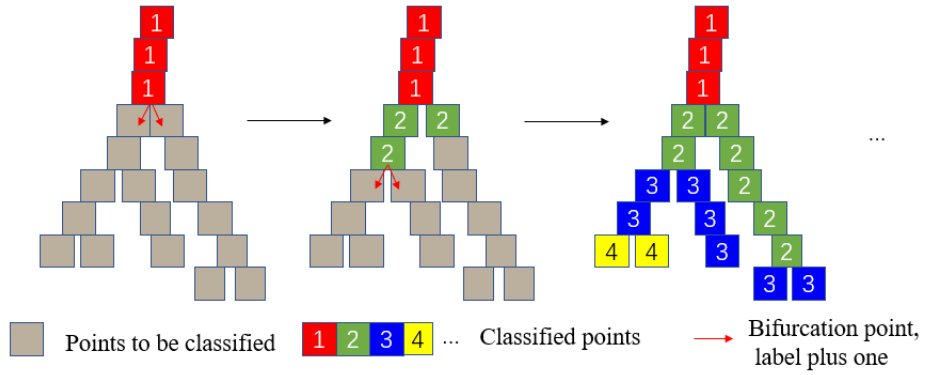

FIGURE 7. Centerline classification algorithm flowchart.

For example, in Figure 6(b), the distance between P1 and P2 represents the length of the tracheal branch between the two points. Because the centerline needs to be extracted in airway classification, the branches originally belonging to the same level could be divided into different bifurcation points, which results in the overall error of airway classification of this branch. Therefore, the introduction of bifurcation buffer length is used to tackle this problem.

IV. EXPERIMENTS

A. EXPERIMENTAL SETUP

The proposed model trains 500 generations on NVIDIA GeForce GTX 1080 with 8GB memory. The Dice similarity function is used in the training loss function. The initial learning rate is set to 0.001. We use SGD(stochastic gradient descent) algorithm as the optimizer. The training set contains 80 data, the validation set contains 10 data, and the test set contains 10 data.

B. QUANTITATIVE EVALUATION METRICS

The performance of model segmentation is tested on clinical data test set and EXACT'09 test data set, and the performance of classification is tested on clinical data test set. Quantitative evaluation metrics of segmentation test include Dice similarity coefficient as expressed in Formula (1) and EXACT'09 official evaluation indicators. The similarity coefficient is based on the labelling results of clinical experts. The evaluation metrics of EXACT'09 for implementation and use are listed in Table 1. Classification performance evaluation mainly refers to the evaluation metrics standard in [13]. The detection rate of each airway level and the classification accuracy of segmental bronchus are evaluated by thoracic radiologists with more than 10 years of clinical experience.

$$Dice = \frac{2|X \cap Y|}{|X| + |Y|} \tag{1}$$

where X represents the ground truth mask and Y represents the predicted mask result. The coefficient 2 in the molecule is due to the repeated calculation of common elements between X and Y by denominator.

C. AIRWAY SEGMENTATION INTEGRITY EXPERIMEN

This experiment is mainly used to verify the integrity of airway segmentation. The 10 airway ground truth used in the test are obtained by using the method in Section 2. Table 2 gives the complete results of this experiment, in which the average Dice is 0.9032. The average number of airway branches is 215.7, and the detection rate of airway branches is 86.63%. The total length of airway tree is 394.9 cm, with an average leak of 8207.9 voxel pixels and the false positive rate is

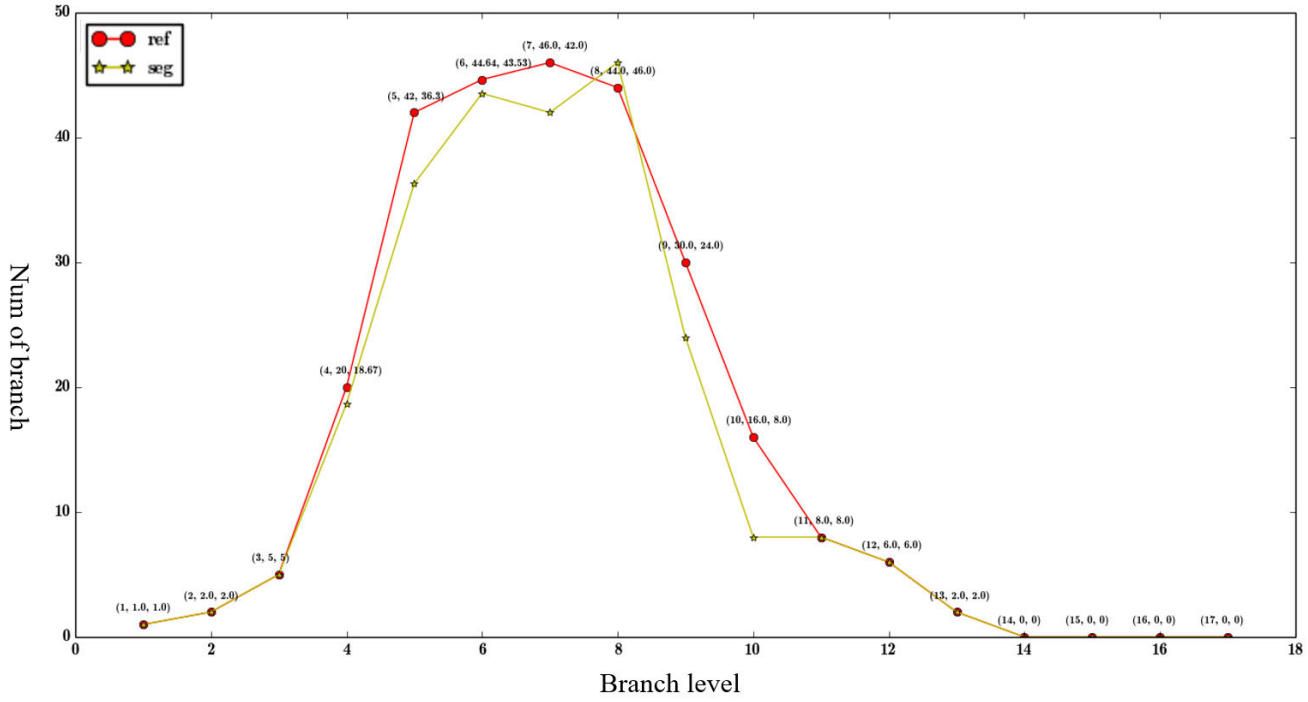

FIGURE 8. Number of bronchial detection at different levels.

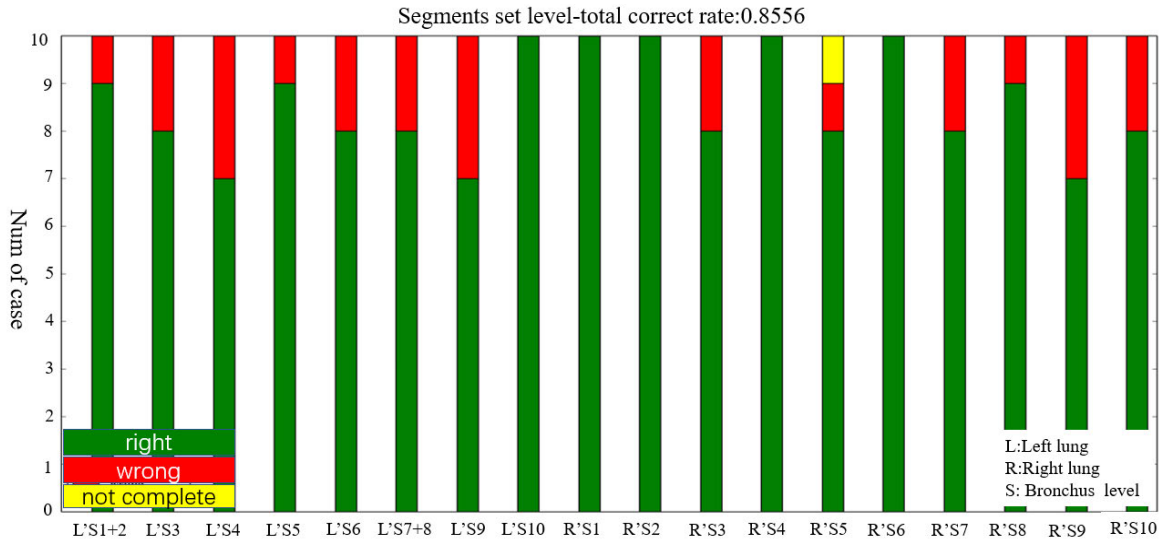

FIGURE 9. Number of bronchial detection at different levels.

1.44%. The first and third row in Figure 10 are visualization of comparisons between segmentation results and doctor's gold standard, in which the green area is the overlap area between the segmentation result and the ground truth, and the red area is the false positive leakage area relative to the gold standard.

D. AIRWAY CLASSIFICATION EXPERIMENT

This experiment is mainly used to verify the detection rate of bronchus and classification accuracy at each level. The rate of detection in each level is determined by the clinicians.

In 10 cases, the detection results of each level of bronchus are shown in Figure 8. In Figure 8, the abscissa represents the level of the airway branch (the level of the branch equals to the label of the classified airway), and the ordinate represents the number of branch levels. And *ref* in red indicates the average number of bronchus in the gold standard in the total test data set, *seg* in yellow indicates the average number of bronchus in the classified results in the total test data set. The detection rate is set to *seg/ref*. Main airway (label 1), left and right bronchus (label 2) and lung bronchus (label 3) are classified correctly and the detection is complete, the average number of correct classification of bronchial bronchus (label

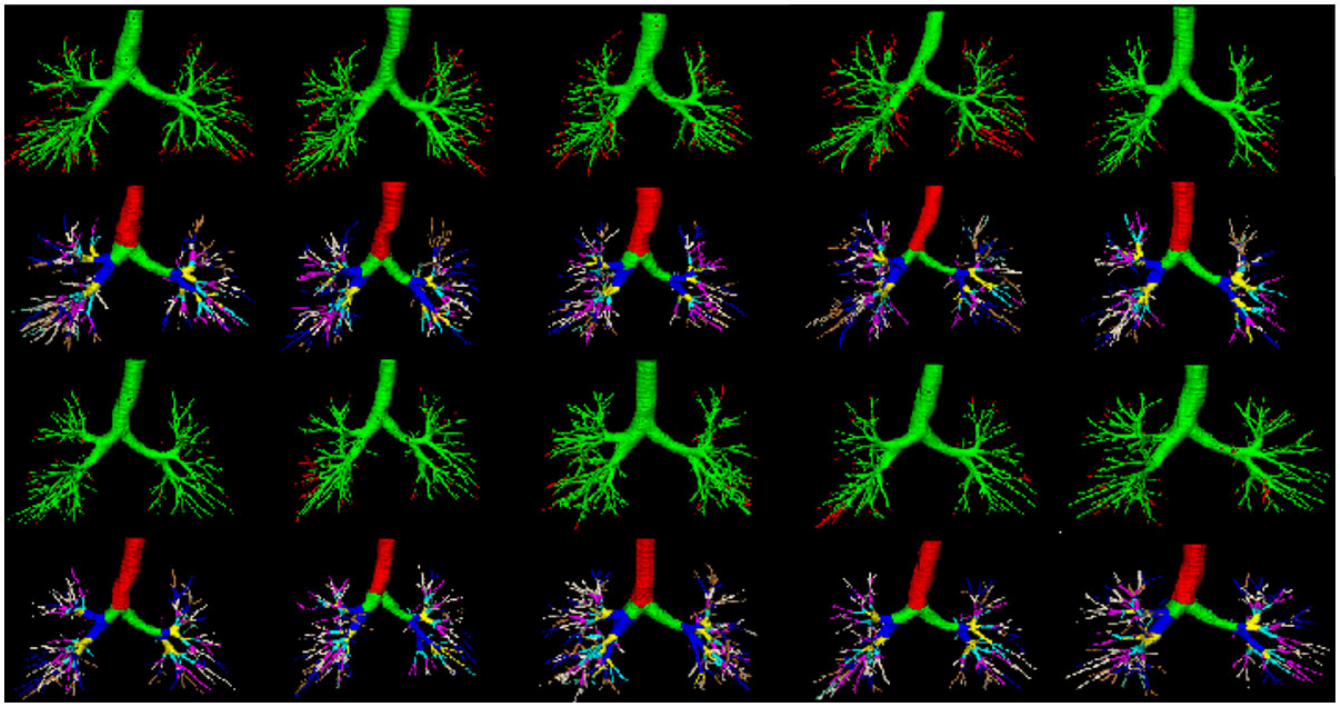

FIGURE 10. Segmentation and classification results in our own test data, (1) green: true positive, red: false positive, in 1st and 3rd row. (2) colormap refer to Figure6, in 2nd and 4th row.

TABLE 1. Description for measurement.

Measurement	Description
Branch count	The number of branches that are detected correctly
Branch detected	The fraction of branches that are detected, with respect to the total number of branches present in the reference
Tree length	The sum of the length of the centerlines of all correctly detected branches
Tree length detected	The fraction of tree length that is detected correctly relative to the reference
Leakage count	The number of disconnected sources where leakage occurs (26 connectivity)
Leakage volume	The volume of regions that are not marked as "correct" in the reference
False positive rate	The fraction of total segmented volume that is not marked as "correct" relative to the reference

4) is 18.67, the detection rate is 93.35%, the average number of subsegmental bronchi (label 5) is 36.3, the detection rate is 86.4%. The airway after the segmental bronchus has a large number of branches and is very thin, making statistics difficult, so the subsequent statistical results are for reference only.

Figure 9 shows the left and right segment bronchus classification accuracy. If the corresponding bronchus level is classified correctly, it will be regarded as 'RIGHT', if the classification is wrong, it will be regarded as 'WRONG', and if it is not segmented, it will be regarded as 'NOT COMPLETE'. When evaluating, we count the results of the left and right lung bronchus separately. Then we calculate an overall classification accuracy score based on this statistics result. In this experiment, the average bronchus classification accuracy rate is 85.56%. In Figure 9, the 'L' on the abscissa represents Left Lung, and 'R' represents Right Lung. 'S' represents the bronchus level. For example, 'S1' represents the bronchus labeled in 1, 'S2' represents the bronchus labeled in 2, and so on.

The second and fourth rows in Figure 10 show the airway classification results of 10 test data. In second and fourth rows, different colors represent different level of airway which can refer to the colormap in Figure 6.

E. EXPERIMENTS ON OPEN DATA SET FOR AIRWAY SEGMENTATION

In order to further test the performance of the segmentation model algorithm, we test our model on 20 test datasets published in EXACT'09 Challenge. The 20 test datasets have different scan thickness, reconstruction algorithm and interstitial lung disease with different severity. The model test results include seven performance metrics mentioned in [13]. Table 3 summarizes the performance of different algorithms on the 20 test data of the EXACT'09 Challenge, from which we can see the proposed network has the best performance in many aspects, such as branch count, branch detected and tree length, compared with other algorithms. Table 4 summarizes the computed performance measures of our method in the 20 test cases of EXACT'09. Figure 12 is the result of comparison

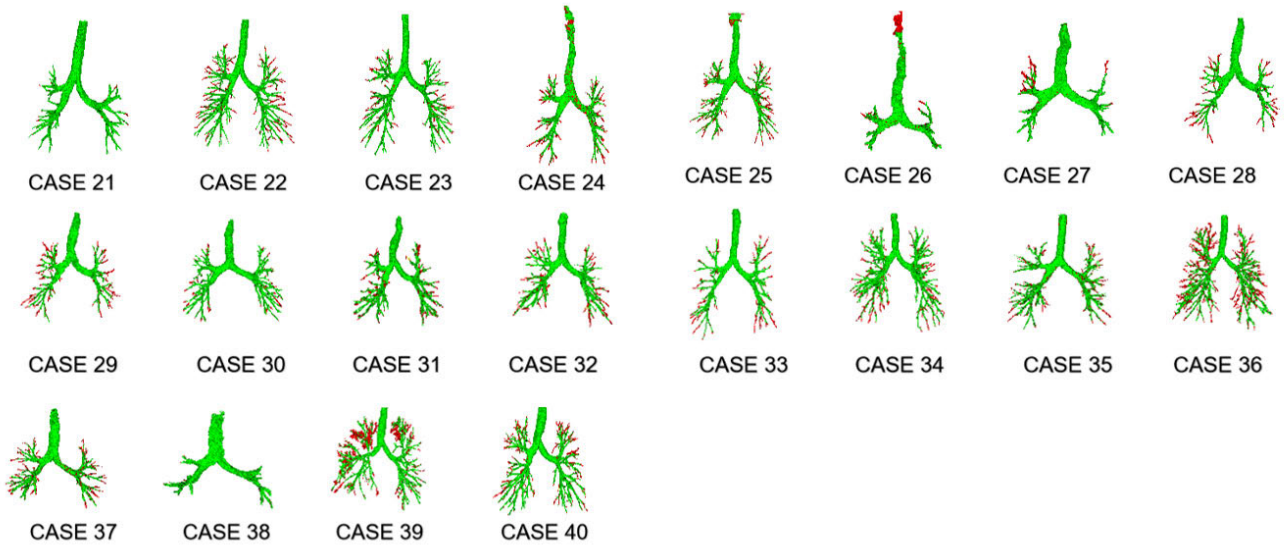

FIGURE 11. Segmentation results in EXACT'09 test data (green: true positive, red: false positive).

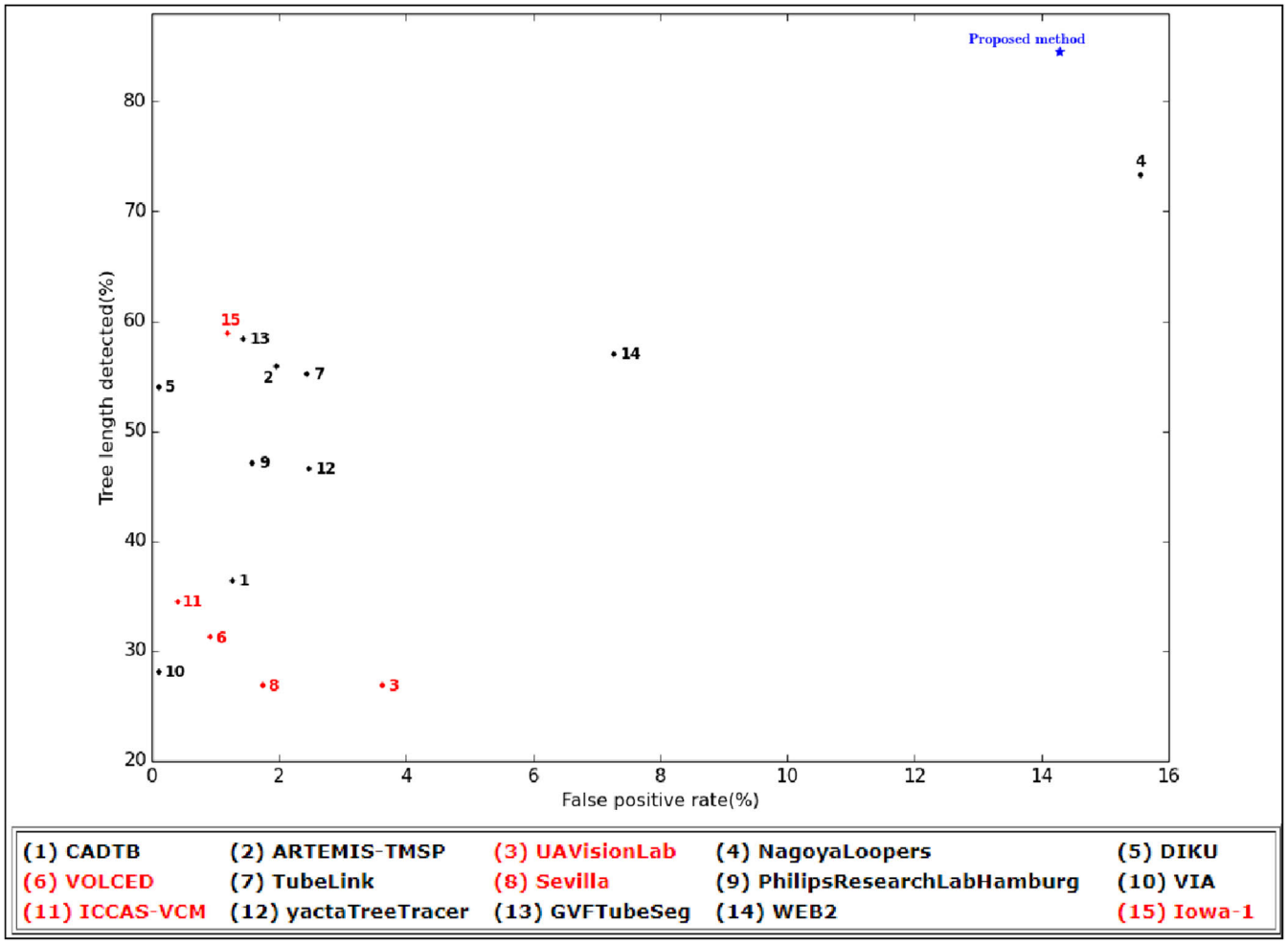

FIGURE 12. EXACT'09 comparison results from 15 segmentation Algorithms.

with 15 algorithms which is officially given by EXACT'09 after submitting our segmentation results. Among them, the detection rate of airway branch is 84.9%, the detection rate of airway tree length is 84.5% and the false-positive rate is 14.29%. Although the false-positive rate is slightly higher, the airway tree length is considerably higher. The degree of

TABLE 2. Result on our own test data.

Test Data Set	Dice	Branch count	Branch detected(%)	Tree length(cm)	Leakage volume(mm^3)	False positive rate(%)
1	0.8790	164	66.39	331.5	4267	0.99
2	0.8912	137	82.53	240.4	8851	2.53
3	0.9313	126	96.92	259.2	9794	2.56
4	0.9066	183	86.72	344.5	6436	1.45
5	0.9282	317	95.48	608.1	12258	1.23
6	0.9216	348	87.87	571.2	11028	1.06
7	0.8926	212	91.37	437.3	7376	1.21
8	0.9162	213	87.29	407.0	7095	1.24
9	0.8964	270	95.74	470.8	8414	1.29
10	0.8692	187	76.01	279.4	6560	0.92
Mean	**0.9032**	**215.7**	**86.63**	**394.9**	**8207.9**	**1.44**

TABLE 3. Comparison of our method and the EXACT'09 methods.

	Branch count	Branch detected(%)	Tree length(cm)	Tree length detected(%)	Leakage count	Leakage volume(mm^3)	False positive rate(%)
CADTB[13]	91.1	43.5	64.6	36.4	2.5	152.3	1.27
ARTEMIS-TMSP[13]	157.8	62.8	122.4	55.9	12.0	563.5	1.96
UAVisionLab[13]	74.2	32.1	51.9	26.9	4.2	430.4	3.63
NagoyaLoopers[13]	186.8	76.5	158.7	73.3	35.5	5138.2	15.56
DIKU[13]	150.4	59.8	118.4	54.0	1.9	18.2	0.11
VOLCED[13]	77.5	36.7	54.4	31.3	2.3	116.3	0.92
TubeLink[13]	146.8	57.9	125.2	55.2	6.5	576.6	2.44
Sevilla[13]	71.5	30.9	52.0	26.9	0.9	126.8	1.75
PhilipsResearchLab Hamburg[13]	139.0	56.0	100.6	47.1	13.5	368.9	1.58
VIA[13]	79.3	32.4	57.8	28.1	0.4	14.3	0.11
ICCAS-VCM[13]	93.5	41.7	65.7	34.5	1.9	39.2	0.41
yactaTreeTracer[13]	130.1	53.8	95.8	46.6	5.6	559.0	2.47
GVFTubeSeg[13]	152.1	63.0	122.4	58.4	5.0	372.4	1.44
WEB2[13]	161.4	67.2	115.4	57.0	44.1	1873.4	7.27
Iowa-1[13]	148.7	63.1	119.2	58.9	10.4	158.8	1.19
Xu[27]	128.7	51.7	94.8	44.5	8.6	1213	0.85
Charbonnier [28]	-	65.4	-	-	-	-	1.68
Lee [29]	158.7	64.9	121.7	56.9	109.8	1633.0	7.3
Nardelli1 [30]	99.0	41.6	75.1	36.5	4.7	52.4	0.71
Lo [31]	150.4	59.8	118.4	54.0	1.9	18.2	0.11
Weinheimer [32]	130.1	53.8	95.8	46.6	5.6	559.0	2.47
Yun [22]	163.4	65.7	129.3	60.1	94.1	726.4	4.56
Our method	**213.7**	**84.9**	**186.9**	**84.5**	**160.3**	**4396.7**	**14.29**

detection rate exceeds all other 15 algorithms. Table 3 shows the specific comparison between our algorithm and other scholars' performance on the EXACT'09 dataset [22]. Since EXACT'09 did not publicly provide the gold standard of marking, all the results of the test set were submitted to the clinician for judgement. The judgement results show that most of the red areas at the end of airway branch in Figure 11 are identified as bronchus. But in fact, only a small

TABLE 4. Performance of the proposed Method on EXACT'09 challenge data.

	Branch count	Branch detected(%)	Tree length(cm)	Tree length detected(%)	Leakage count	Leakage volume(mm^3)	False positive rate(%)
Mean	213.7	84.9	186.9	84.5	160.3	4396.7	14.29
Std. dev.	110.3	11.8	104.3	10.3	87.2	3609.5	8.16
Min	49	50.0	39.1	59.4	40	170.7	1.82
1st quartile	133	82.8	101.6	78.8	94	1562.6	9.16
Median	184	89.0	161.1	89.9	128	4096.9	14.18
3rd quartile	349	93.2	313.6	93.0	256	6513.7	16.28
Max	402	96.2	383.5	93.3	328	13594.9	36.99

amount of the main airway lateral segmentation results should be judged as false positives. Therefore, it can be concluded that the true false positive rate must be less than the evaluation results given by EXACT'09.

V. CONCLUSION

In this paper, we propose a novel network named TACNet for airway segmentation mainly based on Atrous convolution, which is able to produce competitive results on EXACT'09 public datasets. This model mainly uses Atrous convolution without downsampling to effectively solve the problem of airway scale changes. And we further propose an iterative algorithm to classify the airway based on the tree structure of the airway. Two evaluation factors, named the angle of airway bifurcation and the buffer length of airway bifurcation are designed to evaluate the quality of classified airway. The official statistics of EXACT'09 show that our results currently have the best performance on this data set. Based on the method proposed in this paper, follow-up studies on the measurement of airway related parameters such as airway wall thickness, airway diameter and area can be carried out. Combining the complete lung and lung lobes segmentation, it has great application prospects in digital medical treatment.

REFERENCES

[1] C. Wang, J. Xu, L. Yang, Y. Xu, X. Zhang, C. Bai, J. Kang, P. Ran, H. Shen, F. Wen, and K. Huang, "Prevalence and risk factors of chronic obstructive pulmonary disease in China (the China Pulmonary Health [CPH] study): A national cross-sectional study," *Lancet*, vol. 391, pp. 1701–1706, Apr. 2018.

[2] P. J. Barnes, "Chronic obstructive pulmonary disease," *Clinics Chest Med.*, vol. 35, no. 1, p. 13. Mar. 2014. [Online]. Available: https://www.sciencedirect.com/science/article/abs/pii/S0272523113001809

[3] J. Pu, S. Gu, S. Liu, S. Zhu, D. Wilson, J. M. Siegfried, and D. Gur, "CT based computerized identification and analysis of human airways: A review," *Med. Phys.*, vol. 39, no. 5, pp. 2603–2616, Apr. 2012.

[4] W. Davidson and T. R. Bai, "Lung structural changes in chronic obstructive pulmonary disease," *Curr Drug Targets Inflamm Allergy*, vol. 4, no. 6, pp. 643–649, Jan. 2005.

[5] M. Hasegawa, Y. Nasuhara, Y. Onodera, H. Makita, K. Nagai, S. Fuke, Y. Ito, T. Betsuyaku, and M. Nishimura, "Airflow limitation and airway dimensions in chronic obstructive pulmonary disease," *Amer. J. Respiratory Crit. Care Med.*, vol. 173, no. 12, pp. 1309–1315, Jun. 2006.

[6] K. Kuwano, C. H. Bosken, P. D. Paré, T. R. Bai, B. R. Wiggs, and J. C. Hogg, "Small airways dimensions in asthma and in chronic obstructive pulmonary disease," *Amer. Rev. Respiratory Disease*, vol. 148, pp. 1220–1225, Nov. 1993.

[7] P. Shuang and X. Changyan, "Segmentation of pulmonary airway tree by combining region growing and fuzzy connectedness," *Comput. Eng. Appl.*, vol. 52, no. 13, pp. 201–205, Jul. 2016.

[8] H. E. Rui-Hua, L. U. Jian-Feng, and T. Li-Jun, "Automatic segmentation method for three-dimensional bronchial tree based on active contour model," *Chin. J. Med. Phys.*, vol. 33, no. 1, pp. 68–71, Jan. 2016.

[9] A. Fabijańska, "Two-pass region growing algorithm for segmenting airway tree from MDCT chest scans.," *Comput. Med. Imag. Graph.*, vol. 33, pp. 46–537, Oct. 2009.

[10] Z. Bian, J.-P. Charbonnier, J. Liu, D. Zhao, D. A. Lynch, and B. van Ginneken, "Small airway segmentation in thoracic computed tomography scans: A machine learning approach," *Phys. Med. Biol.*, vol. 63, no. 15, Aug. 2018, Art. no. 155024.

[11] B. Irving, P. Taylor, and A. Toddpokropek, "3D segmentation of the airway tree using a morphology based method," in *Proc. 2nd Int. Workshop Pulmonary Image Anal.*, 2009, pp. 297–307.

[12] P. Lo, J. Sporring, H. Ashraf, J. J. H. Pedersen, and M. de Bruijne, "Vessel-guided airway tree segmentation: A voxel classification approach," *Med. Image Anal.*, vol. 14, no. 4, pp. 527–538, Aug. 2010.

[13] P. Lo, B. Van Ginneken, J. M. Reinhardt, T. Yavarna, P. A. De Jong, B. Irving, C. Fetita, M. Ortner, R. Pinho, J. Sijbers, and M. Feuerstein, "Extraction of airways from CT (EXACT'09)," *IEEE Trans. Med. Imag.*, vol. 31, no. 11, pp. 2093–2107, Nov. 2012.

[14] A. Krizhevsky, I. Sutskever, and G. Hinton, "ImageNet classification with deep convolutional neural networks," *Commun. ACM*, vol. 60, no. 6, pp. 84–90, Jun. 2017. [Online]. Available: https://www.onacademic.com/detail/journal_1000039913864210_2a08.html, doi: 10.1145/3065386.

[15] E. Shelhamer, J. Long, and T. Darrell, "Fully convolutional networks for semantic segmentation," *IEEE Trans. Pattern Anal. Mach. Intell.*, vol. 39, pp. 640–651, 2014.

[16] O. Ronneberger, P. Fischer, and T. Brox, "U-net: Convolutional networks for biomedical image segmentation," in *Proc. Int. Conf. Med. Image Comput. Comput.-Assist. Intervent.*, 2015, pp. 234–241.

[17] F. Milletari, N. Navab, and S.-A. Ahmadi, "V-Net: Fully convolutional neural networks for volumetric medical image segmentation," in *Proc. 4th Int. Conf. 3D Vis. (DV)*, Oct. 2016, pp. 565–571.

[18] A. G.-U. Juarez, H. A. W. M. Tiddens, and M. de Bruijne, "Automatic airway segmentation in chest CT using convolutional neural networks," 2018, *arXiv:1808.04576*. [Online]. Available: http://arxiv.org/abs/1808.04576

[19] D. Jin, Z. Xu, A. P. Harrison, K. George, and D. J. Mollura, "3D convolutional neural networks with graph refinement for airway segmentation using incomplete data labels," in *Proc. Int. Workshop Mach. Learn. Med. Imag.*, 2017, pp. 141–149.

[20] Q. Meng, H. Roth, T. Kitasaka, M. Oda, J. Ueno, and K. Mori, "Tracking and segmentation of the airways in chest CT using a fully convolutional network," in *Proc. MICCAI*, 2017, pp. 198–207.

[21] J.-P. Charbonnier, E. M. V. Rikxoort, A. A. A. Setio, C. M. Schaefer-Prokop, B. V. Ginneken, and F. Ciompi, "Improving airway segmentation in computed tomography using leak detection with convolutional networks," *Med. Image Anal.*, vol. 36, pp. 52–60, Feb. 2016.

[22] J. Yun, J. Park, D. Yu, J. Yi, M. Lee, H. J. Park, J.-G. Lee, J. B. Seo, and N. Kim, "Improvement of fully automated airway segmentation on volumetric computed tomographic images using a 2.5 dimensional convolutional neural net," *Med. Image Anal.*, vol. 51, pp. 13–20, Jan. 2019.

[23] A. Paul Yushkevich, J. Piven, H. C. Hazlett, R. G. Smith, S. Ho, C. J. Gee, and G. Gerig, "User-guided 3D active contour segmentation of anatomical structures: Significantly improved efficiency and reliability," *NeuroImage*, vol. 31, pp. 28–1116, Jun. 2006.
[24] F. Yu and V. Koltun, "Multi-scale context aggregation by dilated convolutions," *CoRR*, vol. abs/1511.07122, pp. 1–13, Nov. 2015.
[25] P. J. Reynisson, M. Scali, E. Smistad, E. F. Hofstad, H. O. Leira, F. Lindseth, T. A. N. Hernes, T. Amundsen, H. Sorger, and T. Langø, "Airway segmentation and centerline extraction from thoracic CT–comparison of a new method to state of the art commercialized methods," *PLoS ONE*, vol. 10, no. 12, Dec. 2015, Art. no. e0144282.
[26] Z. Bian, W. Tan, J. Yang, J. Liu, and D. Zhao, "Accurate airway centerline extraction based on topological thinning using graph-theoretic analysis," *Bio-Med. Mater. Eng.*, vol. 24, pp. 49–3239, Jan. 2014.
[27] Z. Xu, U. Bagci, B. Foster, A. Mansoor, J. K. Udupa, and D. J. Mollura, "A hybrid method for airway segmentation and automated measurement of bronchial wall thickness on CT," *Med. Image Anal.*, vol. 24, no. 1, pp. 1–17, Aug. 2015.
[28] J.-P. Charbonnier, E. M. V. Rikxoort, A. A. A. Setio, C. M. Schaefer-Prokop, B. V. Ginneken, and F. Ciompi, "Improving airway segmentation in computed tomography using leak detection with convolutional networks," *Med. Image Anal.*, vol. 36, pp. 52–60, Feb. 2017.
[29] M. Lee, J. Lee, N. Kim, J. B. Seo, and S. M. Lee, "Hybrid airway segmentation using multi-scale tubular structure filters and texture analysis on 3D chest CT scans," *J. Digit. Imag.*, vol. 32, pp. 1–14, Oct. 2018.
[30] P. Nardelli, K. A. Khan, A. Corvò, N. Moore, M. J. Murphy, M. Twomey, O. J. O'Connor, M. P. Kennedy, R. S. J. Estépar, M. M. Maher, and P. Cantillon-Murphy, "Optimizing parameters of an open-source airway segmentation algorithm using different CT images," *Biomed. Eng. OnLine*, vol. 14, no. 1, pp. 1–24, Dec. 2015.
[31] P. Lo, J. Sporring, and M. D. Bruijne, "Multiscale vessel-guided airway tree segmentation," *Med. Image Anal.*, vol. 14, pp. 527–538, Sep. 2009.
[32] O. Weinheimer, T. Achenbach, and C. Düber, "Fully automated extraction of airways from CT scans based on self-adapting region growing," *Comput. Tomogr.*, vol. 27, no. 1, pp. 64–74, 2009.
[33] Y. Qin, M. Chen, H. Zheng, Y. Gu, M. Shen, J. Yang, X. Huang, Y.-M. Zhu, and G.-Z. Yang, "AirwayNet: A voxel-connectivity aware approach for accurate airway segmentation using convolutional neural networks," in *Proc. Med. Image Comput. Comput. Assist. Intervent. (MICCAI)*, Shenzhen, China, 2019, p. 1.
[34] Y. Qin, Y. Gu, H. Zheng, M. Chen, J. Yang, and Y.-M. Zhu, "AirwayNet-SE: A simple-yet-effective approach to improve airway segmentation using context scale fusion," in *Proc. IEEE 17th Int. Symp. Biomed. Imag. (ISBI)*, Iowa City, Iowa, Apr. 2020, pp. 809–813.

GUOHUA CHENG received the master's degree from the Nanyang University of Technology, Singapore. He is currently pursuing the Ph.D. degree with Fudan University, Shanghai, China. Since 2012, he has been a CEO of Jianpei Technology Company Ltd., a 1000 Talents Plan Member of Zhejiang Province, a 521 Program Member of Hangzhou city, a Chairman of the Organizing Committee of the West Lake International Medical Forum, a Deputy Leader of the Big Data and Artificial Intelligence Group with the China Research Hospital Association, the Director of Digital China Industry Development Alliance, the Artificial Intelligence Committee of China Association for Medical Device Industry and the Chinese Innovative Alliance of Industry Education, Research and Application of Artificial Intelligence for Medical Imaging (CAIERA), a Vice President of the Artificial Intelligence Alumni Association of Shanghai Jiaotong University, and an Executive Director of the Hangzhou Association for Artificial Intelligence. He is also works on medical image artificial intelligence. His current interests include machine learning and biomedical engineering.

XIAOMING WU is currently a Chief Physician, an Associate Professor, and a Master of Medicine with The Second Affiliated Hospital of Zhejiang University School of Medicine, engaged in imaging and interventional medicine. He is also a member of the Respiratory Imaging Professional Committee of the Respiratory Branch of the Chinese Medical Doctor Association, a Standing Member of the Imaging Diagnosis Branch of the Zhejiang Anticancer Association, and a member of the Imaging Branch of the Zhejiang Association of Integrative Medicine. He edited two monographs and won one third prize of Provincial Science and Technology Progress Award.

WENDING XIANG received the Ph.D. degree from the Institute of Optoelectronics, Chinese Academy of Sciences, in 2019. He is currently engaged in deep learning of medical imaging. His research interests include artificial intelligence and natural image processing.

CHUAN GUO received the bachelor's degree from the Zhejiang University School of Medicine. He is currently the Deputy Chief Physician with the Department of Radiology, Zhejiang Integrated Traditional Chinese and Western Medicine Hospital, and a member of the National Imaging Technology Management Committee.

HONGLI JI received the Ph.D. degree from Nanyang Technological University, Singapore. He is currently one of the Founder of Hangzhou Jianpei Technology Company Ltd. His research interests include computer vision and big data analysis of medical images.

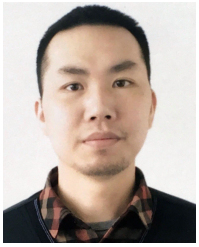

LINYANG HE received Ph.D. degree from the University of Chinese Academy of Sciences, Beijing, China, in 2016. He is currently a Research Leader with the Deep Learning Team, Jianpei Technology Company Ltd. His research interests include medical image analysis, computer vision, and artificial intelligence, specifically on the topic of improving lesion detection, anatomical structure segmentation and quantification, cancer diagnosis and therapy, and surgical robotic perception.